Ullage Temperatures in Wet Spent Fuel Transport Flasks.

D J Burt*, A R Cory**, S J Graham** and M Myszko*

* Rose Consulting Engineers Ltd, 17 Home Farm Avenue, Macclesfield, SK10 3QW, UK.
T: +44 (0)1625 501054 M: +44 (0)7908 257196 E: alan@rose-consulting.co.uk
** British Nuclear Fuels plc, Risley, Warrington, Cheshire WA3 6AS, UK
T: +44 1925 830 000 E: anthony.r.cory@bnfl.com

Abstract

Calculation techniques for predicting the thermal and hydrodynamic conditions in spent nuclear fuel transport flasks have recently been extended to include Computational Fluid Dynamic modelling (CFD). This paper outlines the modelling methods used for predicting the thermodynamic conditions in the ullage space of wet transport flasks during normal transport and in a simulated fire event. The calculations include conjugate heat transfer; that is thermal transport through substantive solid volumes enclosing fluid spaces, radiative transport within and without the fuel element arrays, and convective transport with phase change. Fuel pin temperatures have been shown by this method to be lower than previously calculated by other methods. In the worst case considered, representing the highest licensed thermal load in the hottest-running package, pin temperatures have been shown to remain far below temperatures that could cause cladding deterioration or auto-ignition of radiolysis gas products.

Symbols

Cp	Specific heat capacity
H_f	Liquid enthalpy
H_g	Vapour enthalpy
H_{fg}	Enthalpy of vapourisation
M	Total fluid mass in ullage space.
$\dot{m}$	Vapour generation or condensation
P_{sat}	Steam partial pressure
R	Universal gas constant
ρ	Density
S	Enthalpy source term
T_{sat}	Vapour Boiling Point
v	Specific volume
Vol	Ullage volume
W	Molecular weight
Y	Mass fraction

Introduction

Spent fuel may be transported in flasks without a liquid heat-transfer medium or in flasks containing water to assist the removal of heat from the spent fuel assemblies. These two approaches are accordingly referred to as dry or wet flask transports. It is necessary to ensure that heat transfer is sufficiently effective in order to prevent the peak fuel pin temperatures reaching levels where either degradation of the fuel pin cladding, or auto ignition of combustible gases, could occur.

In the case of dry flasks these conditions are relatively straightforward to calculate. In a wet flask the bulk of the fuel assemblies are cooled by water. However, it is necessary to provide an ullage volume for water expansion, and current package designs have a proportion of the fuel content exposed in the ullage volume. Not only is this fuel less effectively cooled, but accurate analysis of peak temperature is difficult.

Safety case assessments for the transport of spent nuclear fuel have previously used a mixture of conductive and radiative thermal modelling to establish the likely thermodynamic conditions in the flask during normal transport and in fire accident conditions. These techniques are known to be

pessimistic in that fluid convection, and the influence of convected fluid properties are neglected or approximated as simple enhancements to the conductive properties of solid regions. Computational Fluid Dynamic modelling (CFD) is an established technique for solving coupled systems of convection and diffusion referred to as the Navier-Stokes equations for fluid flow but also including the convection and diffusion of enthalpy, turbulence species and individual fluid components. The full equation set for CFD is augmented by constitutive relationships such as the equation of state for an ideal gas mixture or the variation of local properties under the influence of local variables (e.g. *Cp* as a polynomial function of temperature). Thermal radiation may be modelled either integral to the CFD code or as an exchange of thermal boundary and source data between the CFD and radiation solver. The flow in the fuel bundle and in the ullage is driven by natural convection; length and time scales within the bundle suggest a Reynolds number of 38 and a Rayleigh number of 1600. Even in the ullage void regions away from the pin bundle, where the boral plate is a key length scale, $Gr < 0.5E+9$. These measures of flow regime suggest that the system may be treated as a laminar flow [3].

Methods for predicting the thermal and hydrodynamic conditions in spent nuclear fuel transport flasks have recently been extended to include CFD modelling. Several commercial CFD codes are available but not all are able to deal with analyses of this complexity. In this paper we report results produced with both the CFX [1] and Fluent [2] codes.

The following sections describe the methods used for predicting the thermodynamic conditions in the ullage space of wet transport flasks during normal transport and in a simulated fire event. The calculations include conjugate heat transfer; that is thermal transport through substantive solid volumes enclosing fluid spaces, radiative transport within and without the fuel element arrays, and buoyant convective transport with phase change inside the ullage space. Air, steam and radiolytic hydrogen are represented as separate fluid species with independent constitutive relationships.

A solid model, as shown in Figure 1, represents the geometry of a typical flask configuration, in this case the BNFL NTL-11 flask. Planes of symmetry are used to reduce the model to a periodic section and the submerged fuel is represented only as a thermal boundary to the ullage and flask wall. The significant features of the model are the mild steel outer shell, the stainless clad lead liner, the multi element bottle (MEB) and the inner fuel regions with each pin clad in zircaloy and the complete assembly enclosed by a boronated stainless steel lodgement.

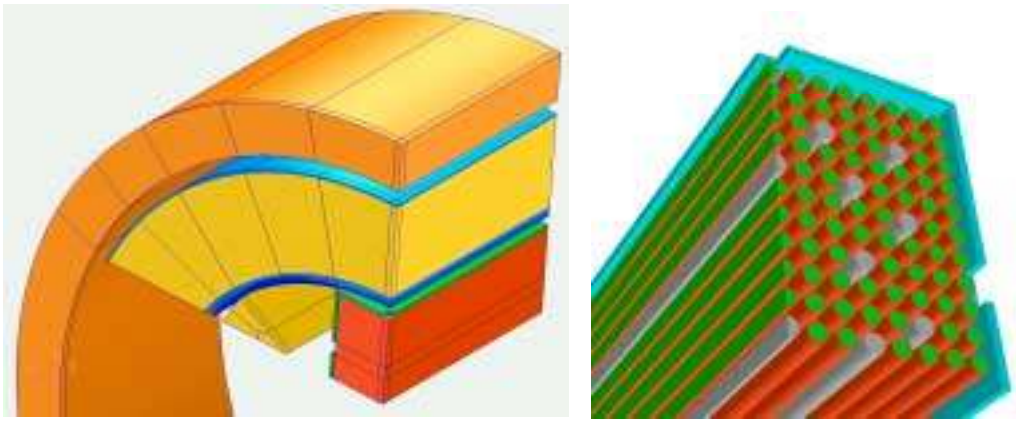

Figure 1: Flask and fuel section solid models. Only the exposed fuel is considered the submerged fuel is modelled as a stratified thermal source.

Geometry and grid generation. A discretised grid of finite volumes was generated within the material boundaries of the solid model. A first study approximated the fuel array with a porous region and used supplementary view factors to inhibit radiative transport in the fuel pin bundle; boundary temperatures from this model were then imposed on a separate explicit fuel pin model. The strong coupling between the radiatively dominated thermal transport in the fuel array and the convective transport in the ullage space could not be correctly accounted for in this un-coupled approach resulting in a significant over prediction of the peak fuel pin temperature. Therefore, a second modelling approach was adopted with a single computational grid combining the fuel pin and ullage models. In Fluent this was achieved by

using a mixed element mesh combining tetrahedral cells in the fuel array with hexahedra in the ullage space. In CFX a structured and embedded hexahedral mesh was used.

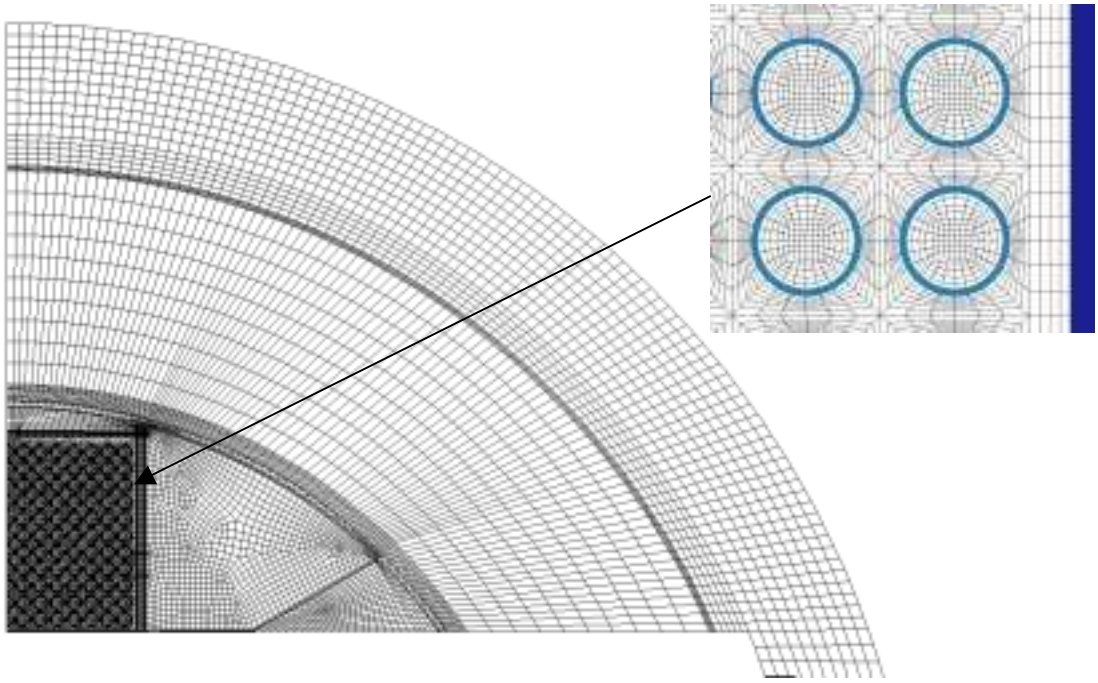

Figure 2: Examples of the mesh cross section including explicit grid of the fuel pin array. Mixed element or unmatched boundary meshes were used to discretise the solid model.

Component models of fluid mixtures. In order to represent the gaseous fluid mixture in the ullage three individual scalar fields were used to define the presence of hydrogen, steam and air. For each component, the fluid properties, *Cp* and *K* were modelled as polynomial functions of the local temperature field. The fluid mixture viscosity did not vary significantly across the range of temperatures considered and was modelled constant while the binary diffusion coefficients for the components of hydrogen and steam in air were kept artificially high in order to promote mixing. The gaseous mixture was modelled as an ideal gas.

Boundary Information. The transport package comprises a finned steel flask closely surrounded by a wood composite neutron shield cover, constraining the air flow around the circumferential fins. For transport on the European rail system, a ventilated aluminium railwagon canopy further encloses the package. The flask itself is a closed system so the boundary conditions used were the volumetric heat generation rate of the fuel pins, the liquid volume saturation temperature and the external finned circumferential wall boundary conditions. In normal transport the internal water surface temperature below the ullage was set as a constant isotherm and the external flask heat transfer coefficient and ambient temperatures were computed in a separate CFD model. Note that, in this case, the fin structures around the outside of the flask were not modelled explicitly but were represented by enhanced external heat transfer coefficients based on fin effectiveness correlations [3]. A worst case was assumed for normal transport with the flask parked in a railway siding under the ventilated canopy.

For the fire simulation, time dependent boundary conditions were used; that is an external fire temperature of $800°C$ was applied at the outer flask wall with a convective and radiative component for 30 minutes duration. The neutron shield cover and rail wagon canopy was assumed destroyed in the fire, and therefore has no consideration in this part of the analysis. Following the fire the flask was allowed to cool in ambient conditions for a further 6 hours. During this time the internal wall temperature boundaries were varied in accordance with a pre-defined heating and cooling cycle for the submerged fuel.

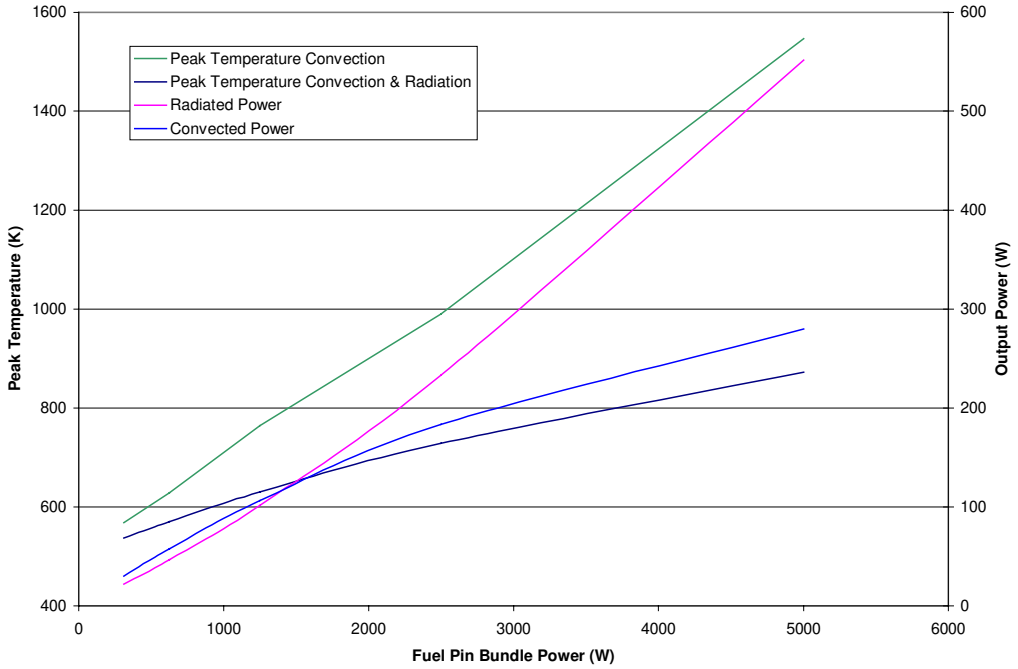

Figure 3: For fuel bundles in isolation the influence of radiative and convective power transfer is investigated. Above 1.5 kW in the bundle the radiative transfer exceeds convective transfer.

Influence of thermal radiation. Sensitivity studies on the influence of thermal radiation and of the model control parameters for the CFD solvers were investigated as part of the study. In particular, for fuel pin arrays in isolation, it was determined that the balance of radiative to convective heat transfer became significantly weighted towards radiation as the thermal power of the fuel was increased. Even for powers less than 500W in the bundle the influence of radiation was significant. Ranges of surface emissivity were also investigated with respect to fuel quality but no attempt was made, in this study, to vary surface fuel and flask emissivities with local temperature.

Pressurisation and de-pressurisation through adding and subtracting mass. A technique for explicitly predicting pressure in normal operation was established and extended to the fire accident scenario where steam evaporation and condensation was also considered as part of the thermodynamic cycle. In all cases the steam partial pressure was deduced as a function of the ullage saturation temperature, that is the temperature at the surface of the water. During the fire simulation a steam source was applied above the water surface consistent with the allowed steam partial pressure. During the cooling phase the steam partial pressure was calculated for the ullage volume but then removed locally from each computational cell as a bulk condensation term. For the steam generation phase the steam enthalpy source terms was derived from knowledge of the mass generation rate and the specific heat capacity. For the steam condensation phase the arguments of Prakash [4] were followed; that is the enthalpy of the condensing vapour was removed from the domain but the latent heat was returned to the domain.

Other modelling techniques were used to establish the saturation temperature as a function of time during the fire event. Given T_{sat} at all time during the fire event it is possible to deduce evaporation and condensation rates for the ullage space as follows;

For the steam component only,

$$Cp = AT_{sat}^2 + BT_{sat} + C$$

where the coefficients of the polynomial are *A*=5.856E-4, *B*=0.10674 and *C*=1789.6.

The heat up phase of the fire occurs over a fixed time period Δt during which the saturation temperature increases almost linearly in the ullage space. From steam tables the vapour specific volume can be deduced for the given saturation temperature such that a steam evaporation rate can be calculated as;

$$\dot{m}_e = \frac{\left(\frac{1}{v_t} - \frac{1}{v_0}\right) Vol}{\Delta t}$$

and the incoming steam vapour enthalpy source in the CFD model is

$$S = \dot{m}_e H_g = \dot{m}_e \, Cp(T_{sat} - T_{ref})$$

For the cooling phase a steam saturation pressure is first calculated as a function of the saturation temperature from a steam table fit

$$P_{sat} = \alpha \exp\left(\beta_1 - \frac{\beta_2}{T_{sat} - \beta_3}\right)$$

where, α = 133.35, β_1=18.3036, β_2=3816.44 and β_3=46.13 for temperature in *K* and pressure in *Pa*.This is used to calculate a steam density,

$$\rho = \frac{P_{sat} W}{R \; T_{sat}}$$

From which the change in mass for a given time step can be calculated with the existing mass of steam, the existing mass fraction and the ullage volume;

$$\dot{m} = \frac{Y M - \rho Vol}{\Delta t}$$

and the steam vapour enthalpy sink in the CFD model is,

$$S = \dot{m} H_f = \dot{m}\left(H_{fg} - H_g\right)$$

that is $Su = \dot{m} H_{fg}$ and $Sp = -\dot{m}$ with the enthalpy of evaporation being derived from a fit to steam table data.

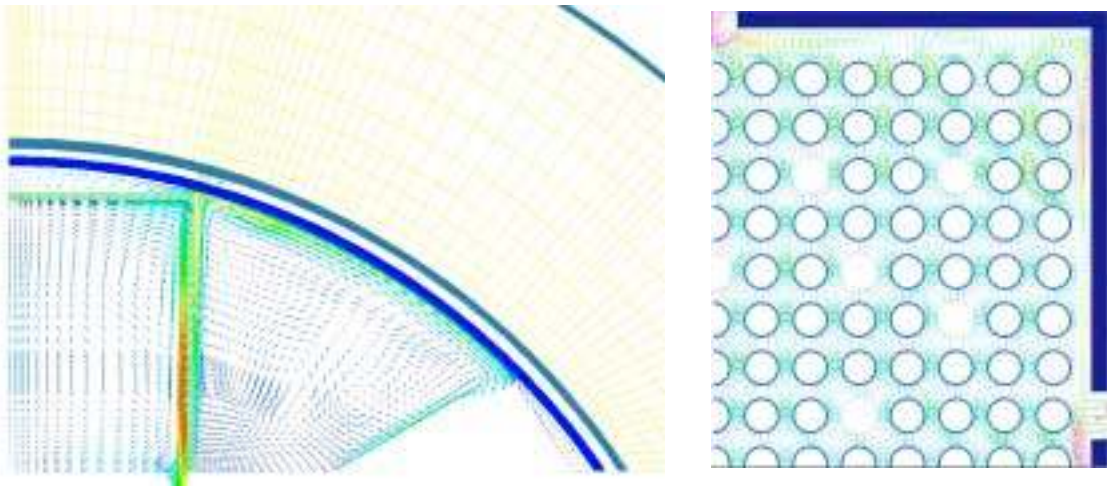

Figure 4: Buoyant convective flow patterns for the ullage space in normal transport. Fuel is modelled as a porous region in the left hand figure.

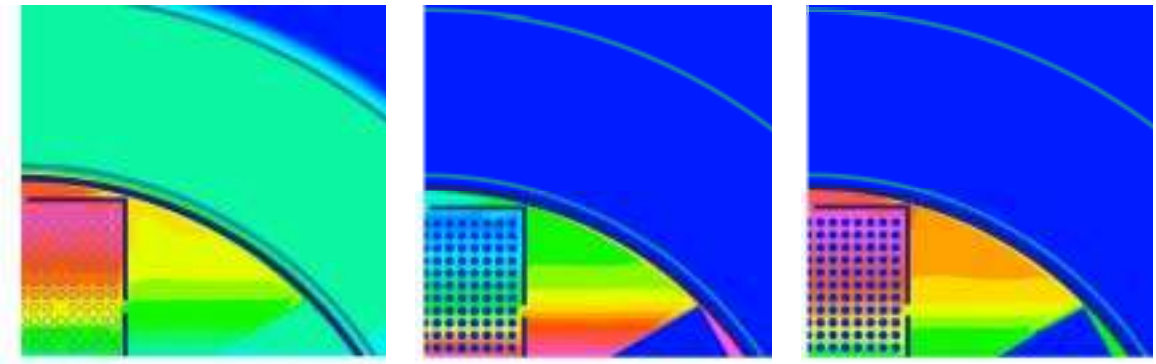

Figure 5: Temperature, density and *Cp* variation in the Ullage space for normal transport.

Buoyancy driven flow patterns. Given that previous safety case studies for transport flasks have tended to rely on conductive and radiative prediction only, it is important to consider the additional convective and constitutive information that the CFD study can provide. We see two significant buoyant recirculations in the modelled regions consistent with the temperature and density plots. The colder and heavier gas is falling to the ullage space floor with heated gas rising through the fuel pins. The boronated stainless steel lodgement enclosing the fuel array is effectively a counter current heat exhanger between the hot fuel zone and the cooler ullage space. The convective influence determines that the hottest pins are near to the top of the fuel bundle as opposed to a purely radiative analysis that would show the hottest pin in the very centre of the bundle. Note that ρ and *Cp* are functions of temperature and mixture fraction.

Thermal History . The most significant finding of the work relates to the influence of vapour in the ullage on the bulk fluid temperature and the maximum pin temperature. The use of a three fluid component model allows the introduction and removal of steam into and out of the ullage volume. In this way, the ullage mass varies in line with the water surface saturation temperature (an applied boundary condition). Earlier studies at fixed internal pressure but exposed to the fire and cool down thermal cycle showed gradual warming of the fuel pins with peak pin temperatures rising $60^{\circ}C$ above normal operation some 4 hours after the fire event. The evaporation and condensation in this model promotes additional convective transport and subsequent cooling during the fire event such that the fuel

pin maximum temperature never exceeds the normal operating condition. This process is illustrated in Figure 6.

Verfification and Validation, A major concern with all mathematical modelling techniques is the agreement between computed data and the real physical system. Extensive work has been done by BNFL to achieve good correlation between experimental data and computed prediction. Much of this work dates back to the early 1980's [5]. A benchmark validation study has recently been completed comparing CFD results, with temperature profiles in a controlled assembly of heated pins. Results of these comparisons [6] are beyond the scope of this paper but generally CFD predictions fall within bands of experimental error when care is taken in the application of both grid resolution and material property data.

Verification is the comparison of method. In this study we used two commercial CFD codes, CFX and Fluent in order to compare temperature distributions and pressure predictions. Our results show that for normal transport at peak thermal loading, CFX and Fluent predict maximum fuel pin temperatures to within 3.5% agreement. The predictions of lead liner temperature agree within 1% and the fin root temperatures agree within 7.3%. CFX temperature predictions are consistently higher than Fluent. For the fire transient the CFX peak pressure prediction is 2.6% higher than the Fluent prediction but 4.3% lower that that obtained by a simple hand calculation.

Conclusion

A model of radiative, convective and conductive/conjugate heat transfer in the ullage space of a spent nuclear fuel transport flask has been constructed with transient thermal boundary conditions simulating a fire event. Sensitivity to model parameters and the influence of different thermal transport mechanisms have been assessed. It is seen that mass transfer within the ullage space has a significant influence on the peak fuel element temperature where additional steam serves to cool the pins below the normal operating temperature even as the bulk ullage gas temperature rises during a simulated fire event.

Fuel pin temperatures have been shown by this method to be lower than previously calculated by other methods. In the worst case considered, representing the highest licensed thermal load in the hottest-running package, pin temperatures have been shown to remain far below temperatures which could cause cladding deterioration, and much below the temperature at which auto-ignition of radiolysis gas products could occur. The safety margins observed being approximately 200 and 150°*C* respectively. These margins are significantly higher than those shown in previous assessments.

Temperatures of MEB components in the ullage region have also been established, as have temperatures of gases in the ullage region. The analysis has also provided a corroboration of maximum package pressures. The overall impact of the CFD analysis has been a considerable enhancement of our knowledge of package thermal behaviour.

References.

1. *CFX4.4 User Manual*, CFX International. Harwell, Oxfordshire, 2001.
2. *Fluent 5.5 User Manuals*, Fluent Europe Ltd, Sheffield UK, 2001.
3. Holman, J.P., *Heat Transfer*, McGraw Hill, 8th Ed, 1999, pp44-55.
4. Prakash, C. *Two Phase Model for Binary Liquid-Solid Phase Change*, Numerical Heat Transfer, Vol 18, p.131.
5. Jones, R.P. *Dry Flask Testing, experimental study to determine the temperature of a horizontal PWR fuel element in a gas filled enclosure*, GEC Energy Systems report ESL/R(81)69, 1981
6. Wilbraham, N. *CFD Analysis of an Experimental Fuel Pin Bundle*, BNFL Internal report RAT 2735, May 2002.

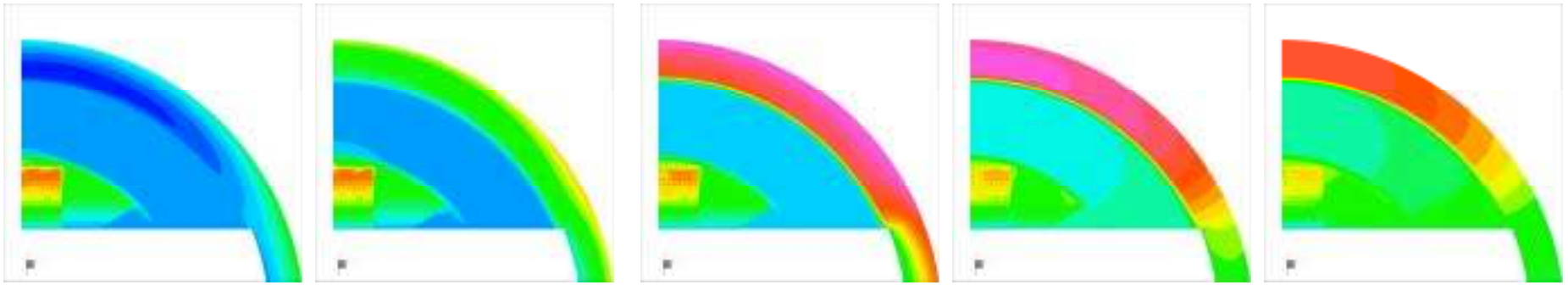

	12.5Minutes	25 Minutes	50 Minutes	74 Minutes
Y_{Steam} 0.69	0.71	0.74	0.78	0.82

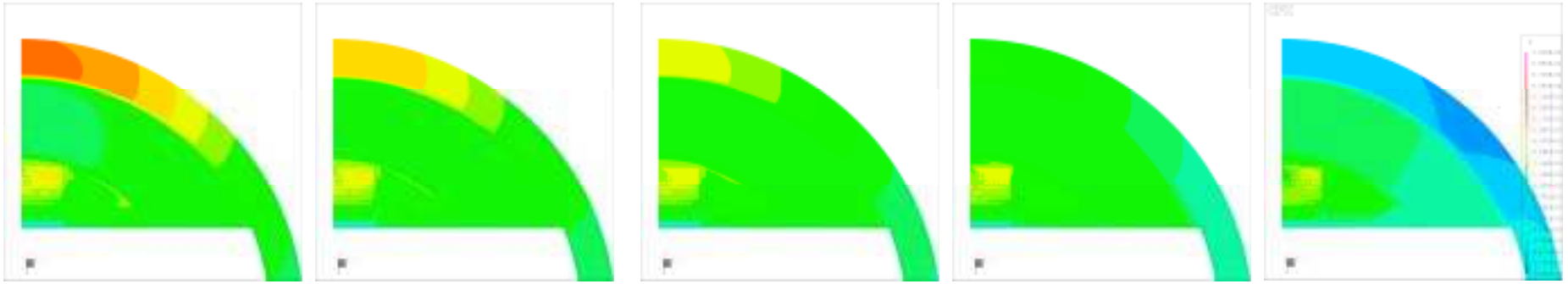

101 Minutes	2 Hours	2.2 Hours	2.8 Hours	4.7 Hours
Y_{Steam} 0.84	0.83	0.825	0.82	0.79

Figure 6: Time temperature sequence for the flask ullage in a simulated fire event. The evaporation, convection and ultimate condensation of steam from the liquid into and out of the ullage space serves to cool the fuel bundle even as the bulk temperature rises.